Thoracic Imaging

3

Javier Campos and Kalpaj R. Parekh

Key Points

- Radiological images play an important role during the evaluation of patients undergoing thoracic surgery.
- Radiological studies must be reviewed, including a posterior–anterior chest radiograph and computed tomography scan of the chest.
- Special emphasis should be given to mediastinal mass with compromise to the airway or great vessels by reviewing the computed tomography scan of the chest.
- Multidetector computed tomography (CT) scan and tracheobronchial reconstruction are more specific studies in the thoracic surgical patient and allow measurements of the airway.
- Magnetic resonance imaging (MRI) provides greater contrast resolution than CT scans and offers the potential for tissue characterization. An MRI is indicated in selected cases, i.e., mediastinal mass with invasion of the superior vena cava.

Introduction

Radiological images play an important role in the preoperative, intraoperative, and postoperative evaluation and diagnosis of patients undergoing thoracic surgery. During the preoperative visit evaluation of the thoracic surgical patient, the clinician must have an understanding of the disease and also become familiar with radiological studies to be able to identify abnormal airway anatomy or compromises to the airway or to use caliper measurements in the tracheobronchial tree if necessary when selecting lung isolation devices. Another important component to a successful preoperative evaluation is an understanding of normal tracheobronchial anatomy. This chapter will be focused on reviewing normal tracheobronchial anatomy and radiological images, with special interest for anesthesiologists involved in the care of the thoracic surgical patient.

Normal Tracheobronchial Anatomy

The trachea is a cartilaginous and fibromuscular structure that extends from the inferior aspect of the cricoid cartilage to the level of the carina [1]. The adult trachea is, on average, 15 cm long. The trachea is composed of 16–22 C-shaped cartilages. The cartilages compose the anterior and lateral walls of the trachea and are connected posteriorly by the membranous wall of the trachea, which lacks cartilage and is supported by the trachealis muscle.

The average diameter in a normal trachea is 22 mm in men and 19 mm in women. In men, the coronal diameter ranges from 13 to 22 mm, and the sagittal diameter ranges from 13 to 27 mm. In women, the average coronal diameter is 10–21 mm and the sagittal is 10–23 mm [2]. The tracheal wall is about 3 mm in thickness in both men and women, with a tracheal lumen that is often ovoid in shape.

The trachea is located in the midline position but often can be deviated to the right at the level of the aortic arch, with a greater degree of displacement in the setting of an atherosclerotic aorta and advanced age or in the presence of severe chronic obstructive pulmonary disease (COPD). With COPD or aging, the lateral diameter of the trachea may decrease with a corresponding increase in the antero-

J. Campos (✉)
Department of Anesthesia, University of Iowa Health Care, Roy and Lucille Carver College of Medicine, Iowa City, IA, USA
e-mail: javier-campos@uiowa.edu

K. R. Parekh
Department of Cardiothoracic Surgery, University of Iowa Hospitals and Clinics, Iowa City, IA, USA

P. Slinger (ed.), *Principles and Practice of Anesthesia for Thoracic Surgery*, https://doi.org/10.1007/978-3-030-00859-8_3

posterior diameter. Conversely, COPD may also lead to softening of the tracheal rings with a decrease in the anteroposterior diameter of the trachea [3]. The cricoid cartilage is the narrowest part of the trachea with an average diameter of 17 mm in men and 13 mm in women.

The trachea bifurcates at the carina into the right and left mainstem bronchus. An important fact is that the tracheal lumen narrows slightly as it progresses toward the carina. The tracheal bifurcation is located at the level of the sternal angle anteriorly and the fifth thoracic vertebra posteriorly. The right mainstem bronchus continues as the bronchus intermedius after the takeoff of the right upper lobe bronchus. In men, the average distance from the tracheal carina to the takeoff of the right upper lobe bronchus is 2.0 cm, whereas it is approximately 1.5 cm in women. One in every 250 individuals from the general population may have an abnormal takeoff of the right upper lobe bronchus emerging from above the tracheal carina on the right side [4]. The diameter of the right mainstem bronchus is an average of 17.5 mm in men and 14.0 mm in women. The trifurcation of the right upper lobe bronchus consists of the apical, anterior, and posterior divisions. The average distance from the tracheal carina to the bifurcation of the left upper and left lower lobe is approximately 5.0 cm in men and 4.5 cm in women. The left mainstem bronchus is longer than the right mainstem bronchus, and it divides into the left upper and the left lower lobe bronchus. The left upper lobe bronchus has a superior and inferior division [5].

Chest Radiographs

The most common study in the patient undergoing thoracic, esophageal, or cardiac surgery is the chest X-radiograph (X-ray). The standard routine chest radiography consists of an erect radiograph made in the posterior–anterior (PA) projection and a left lateral radiograph, both obtained at full inspiration. The normal chest cavity contains four radiographic densities that are easily identified: air, fat, water, and calcium and other metals including bones, granulomas, and vascular calcification. The lungs, which are mostly air and contain some water, blood vessels, bronchi, nerves, lymphatics, alveolar walls, and interstitial tissues, provide the natural contrast that is the basis of chest radiology. When evaluating a chest X-ray, the changes in these densities, which provide natural contrast, are what are observed.

Radiologists in general refer to two regions: the silhouette sign and summation. Depending on the part or parts of the lungs that are involved, the result of this change in the absorption of X-rays is seen by the effect on the normal surface of a hemidiaphragm, for example, or if the descending aorta cannot be seen, then this is an indication that an unusual amount of aerated lung no longer touches the anatomic part. This occurs in part because the alveolar spaces are wholly or partially filled with fluid usually blood, pus, or water or in part because the lung has collapsed and decreased the normal ratio of air and soft tissue. The end result in the latter case would be an increase in opacity which is what the X-ray beam reveals. The heart border and the diaphragm are normally seen because of their interface with aerated lung. When the contiguous lung is not aerated, the opaque tissue of the affected lung blends visually with the soft tissue opacity of the heart, and the heart border is no longer visible. This is what is termed the silhouette sign. Summation by definition is the result of superimposition of many layers of lung tissue, so that the final visual effect is that of a greater amount of tissue in the path of a particular part of the X-ray beam. This is observed when the opacity of fluid in the pleural space, interstitial space, or even lung parenchyma is added on the normal structure of the lung [6]. The most important skill for evaluating a chest X-ray is the knowledge of normal anatomic variants, the specific patterns with pathological changes, and the common signs of abnormal states. Lateral decubitus radiographs are commonly employed to determine the presence or mobility of pleural effusions. These views can also be obtained to detect small pneumothoraces, particularly in patients who are confined to bed and unable to sit or stand erect. A new generation of digital X-ray systems based on flat panel detections is now emerging, and these provide good image quality and very rapid direct access to digital images.

Chest Radiographs and Pulmonary Disease

The basic underlying change in the chest film that allows the detection and diagnosis of abnormalities is usually due to an alteration in lung opacity. This can be caused by technical factors, physiologic variation, or pathologic mechanisms [7]. Diseases that affect the chest can usually be thought of as either those that make the film lighter (increase opacity) or those that make it darker (increase lucency).

For chest disease with increased opacity on radiographs, the conditions that are marked by focal or global increase in the opacity of the film are first examined. These conditions include atelectasis, pulmonary edema, acute respiratory distress syndrome, etc.

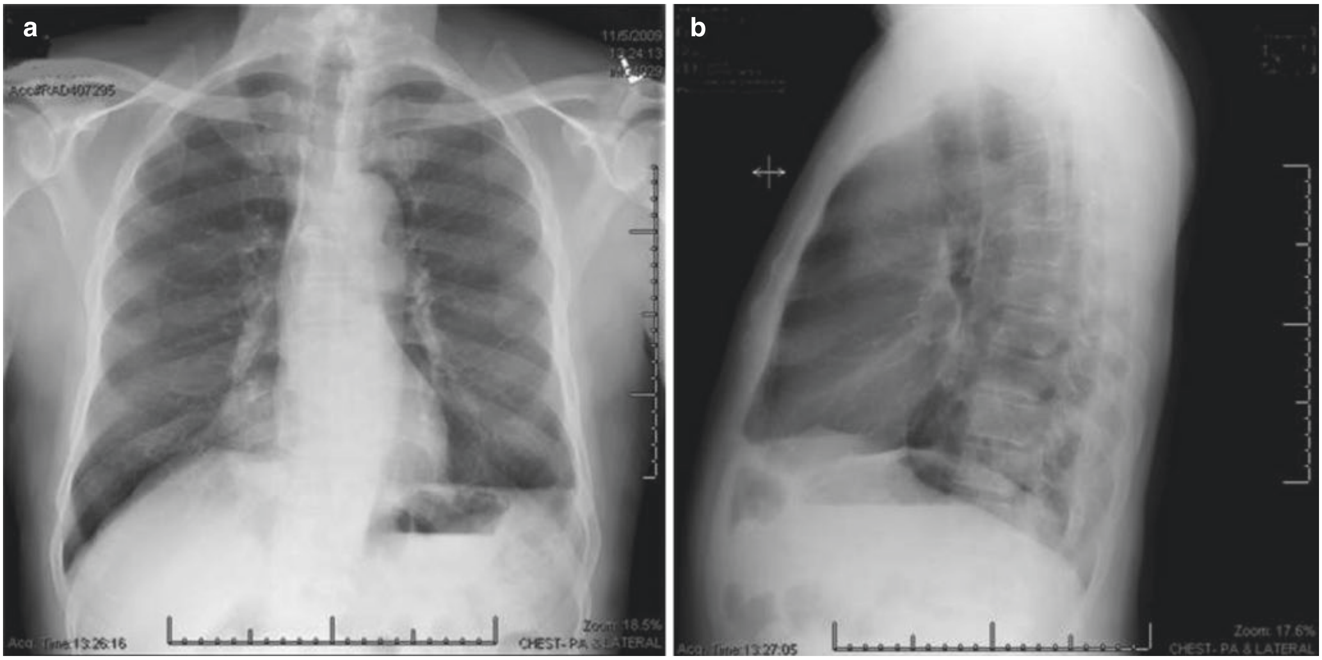

Fig. 3.1 (**a**) Shows a posteroanterior chest radiograph on a 68-year-old male with a lung neoplasm on the right lower lobe. The mass is clearly visible between the 8th and 9th rib on the right hemithorax. (**b**) Shows a lateral chest radiograph showing a round mass on the right hemithorax

Lung Mass and Chest X-Rays

Pulmonary neoplasia presents as opacities on films although usually as a more focal area with varying contours. However, smaller lesions may be very difficult to visualize, particularly when there are overlying bones or other soft tissue. Figure 3.1a shows a posteroanterior chest radiograph on a 68-year-old male with a lung neoplasm on the right lower lobe. The mass is clearly visible between the eighth and ninth rib on the right hemithorax. Figure 3.1b shows a lateral chest radiograph showing a round mass on the right hemithorax.

Mediastinal Mass and Chest X-Rays

In order to understand mediastinal masses and radiological images, it is important to be familiar with the anatomy of the mediastinum. The mediastinum is situated between the two pleural cavities. It extends superiorly from the root of the neck and the thoracic inlet to the hemidiaphragm inferiorly. It is divided into the superior and inferior mediastinum by the transverse thoracic plane, which is an imaginary plane extending horizontally from the sternal angle anteriorly to the border of the fourth thoracic vertebra posteriorly. The inferior mediastinum is subdivided into anterior, middle, and posterior compartments. The anterior mediastinum contains the thymus, trachea, esophagus, vessels, and arteries as well as lymph nodes; any abnormal growth in this region will affect the adjacent area. A mass in this area may compress the tracheobronchial tree and/or major vessels (superior vena cava and pulmonary vessels). The middle mediastinum is the space occupied by the heart and pericardium [8, 9]. Figure 3.2a shows a schematic representation of mediastinal anatomy and Fig. 3.2b a lateral normal radiograph of the chest showing the potential location of mediastinal mass. A variety of neoplasms and other lesions present with anterior mediastinal involvement. Thymoma is the most common primary neoplasm of the anterior mediastinum [10].

Regarding radiological studies in patients with a suspected anterior mediastinal mass, the initial study generally is a standard biplane chest radiography, which will identify up to 97% of mediastinal tumors. The chest X-ray also provides important information regarding the size and the location of the mass [11].

In addition, in this patient group in particular, special attention must be paid to the lateral radiography of the chest to determine the overall extent of the mass and potential involvement of adjacent structures. A barium contrast

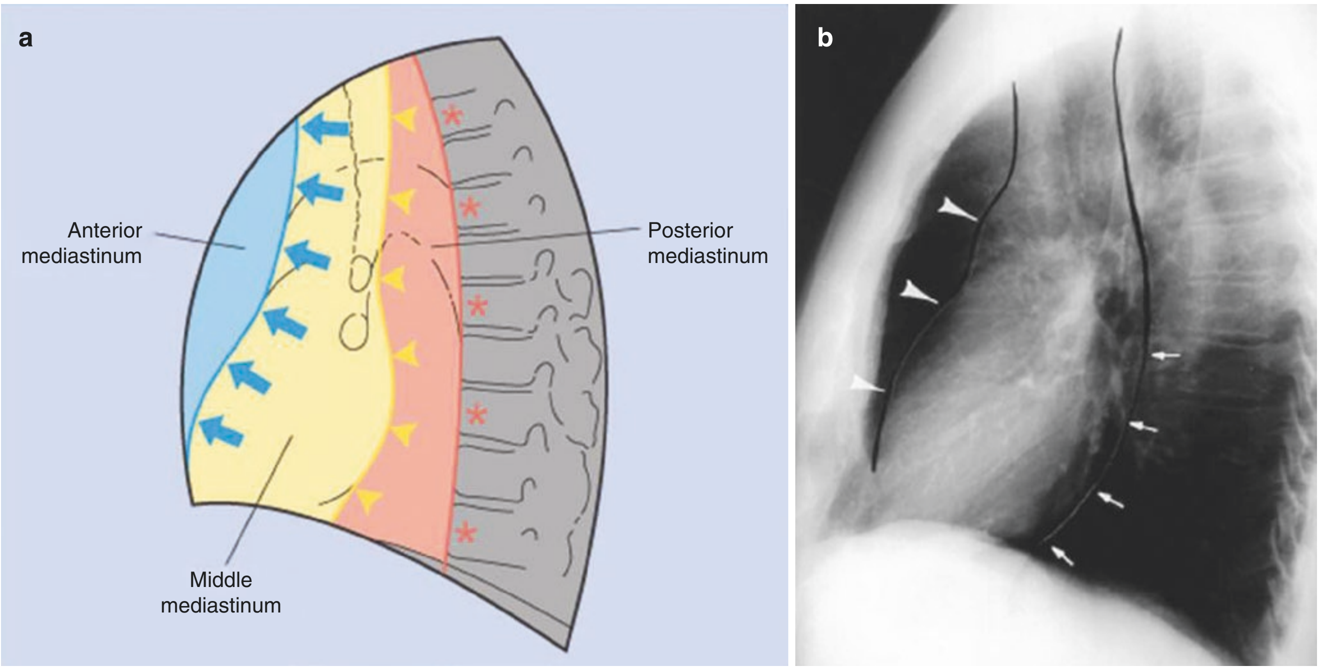

Fig. 3.2 (**a**) Shows a schematic representation of mediastinal anatomy and (**b**) a lateral normal radiograph of the chest showing the potential location of mediastinal mass. (With permission Ref. [10])

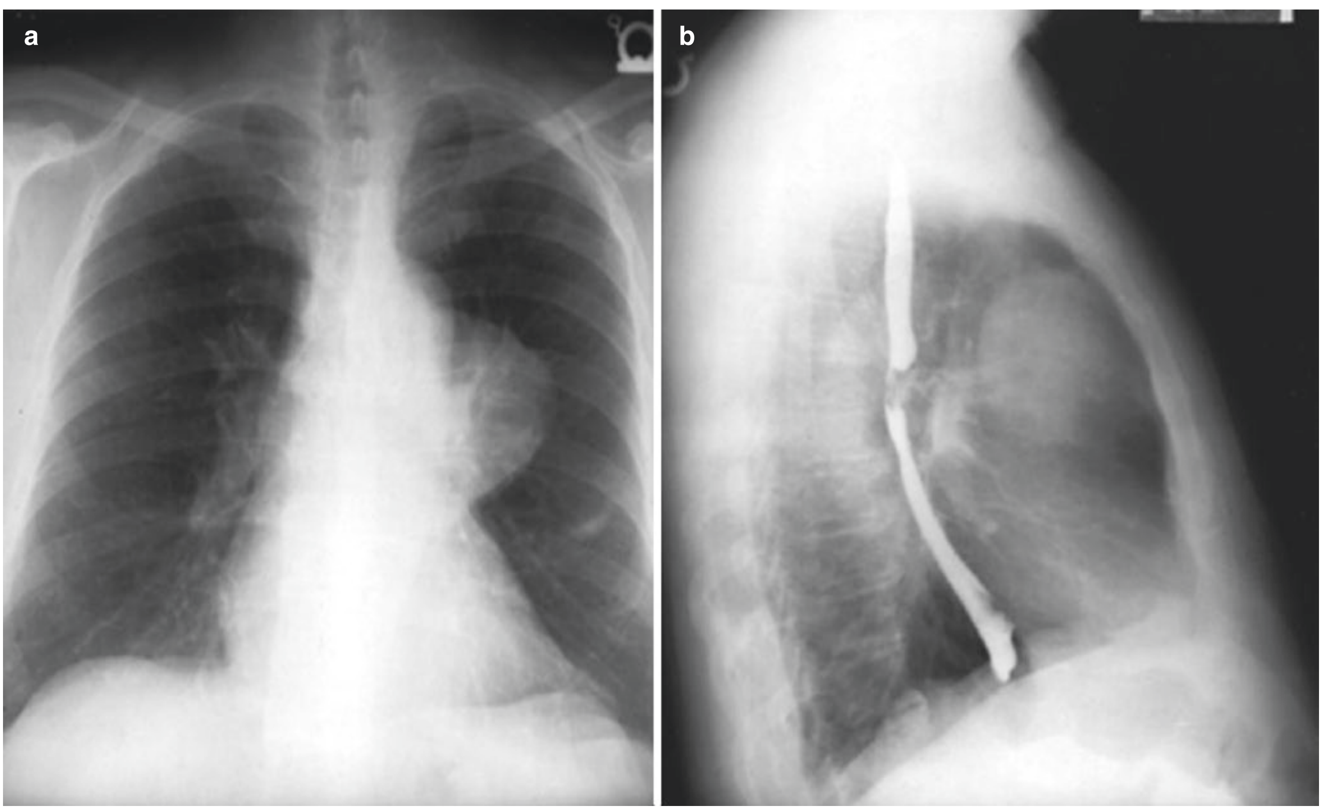

Fig. 3.3 (**a**) Shows an anterior mediastinal mass in the left hemithorax of the posteroanterior chest radiograph. (**b**) Shows a lateral radiograph with esophageal contrast where there is a mediastinal mass without compromise to the tracheobronchial tree

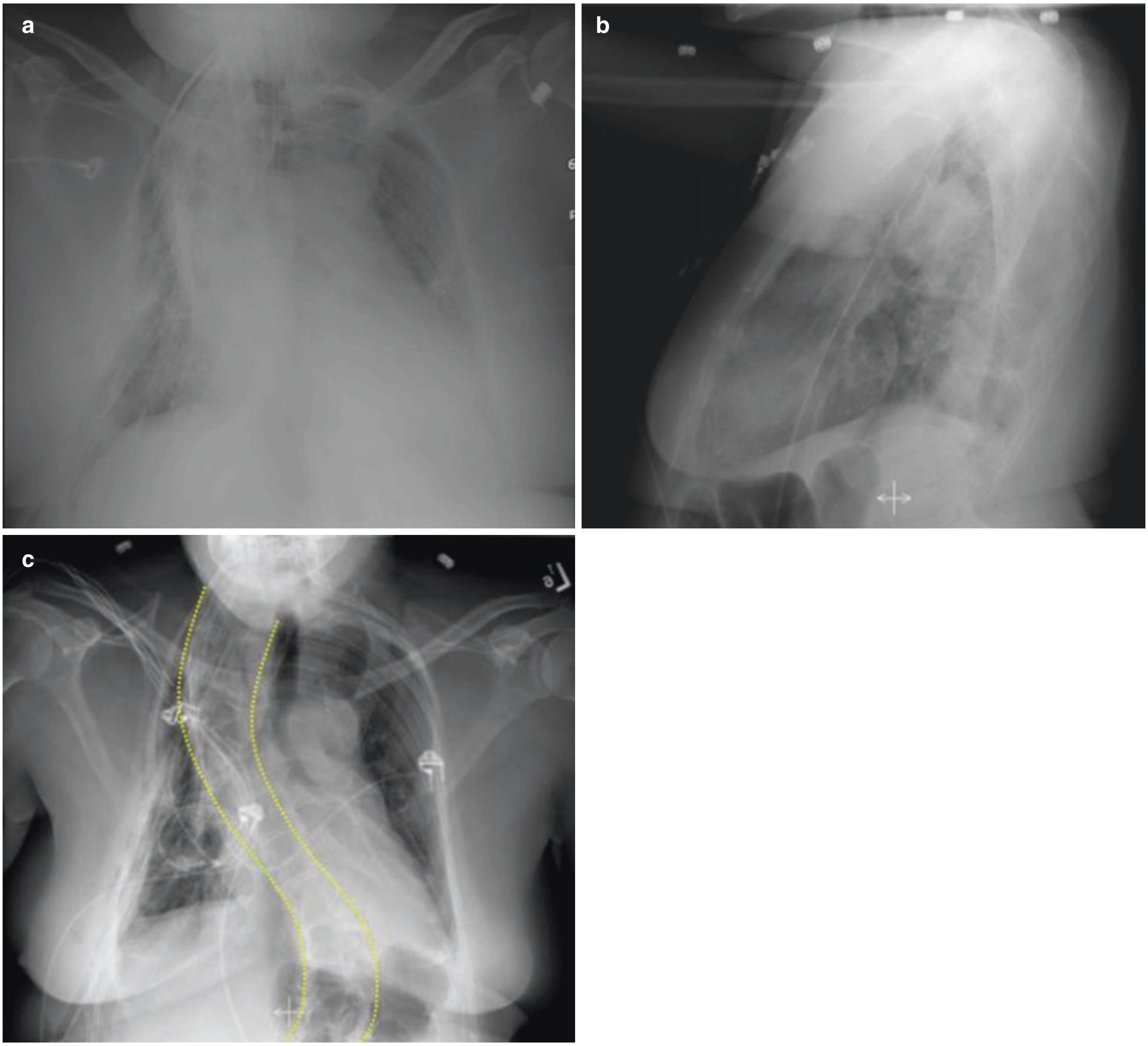

Fig. 3.4 Shows (**a**) a posterior mediastinal mass in the right hemithorax of the posterior–anterior chest radiograph in a female with severe kyphoscoliosis (**b**) a lateral radiograph showing the posterior mediastinal mass, (**c**) a portable posterior–anterior chest radiograph in the post-operative acute care unit after the resection of the posterior mediastinal mass. The yellow dots are showing the contour of the thoracic column showing severe kyphoscoliosis

esophagogram may help to determine whether there is esophageal or tracheobronchial involvement. Figure 3.3a shows an anterior mediastinal mass in the left hemithorax of the posteroanterior chest radiograph. Figure 3.3b shows a lateral radiograph with esophageal contrast where there is a mediastinal mass without compromise to the tracheobronchial tree (Fig. 3.4).

Bullae

Emphysema is characterized by a permanent increase in air spaces distal to the terminal bronchiole beyond the normal size. There is destruction of tissue, leading to a loss of alveolar surface available to participate in air exchange and, sometimes, severe displacement of the adjacent normal lung.

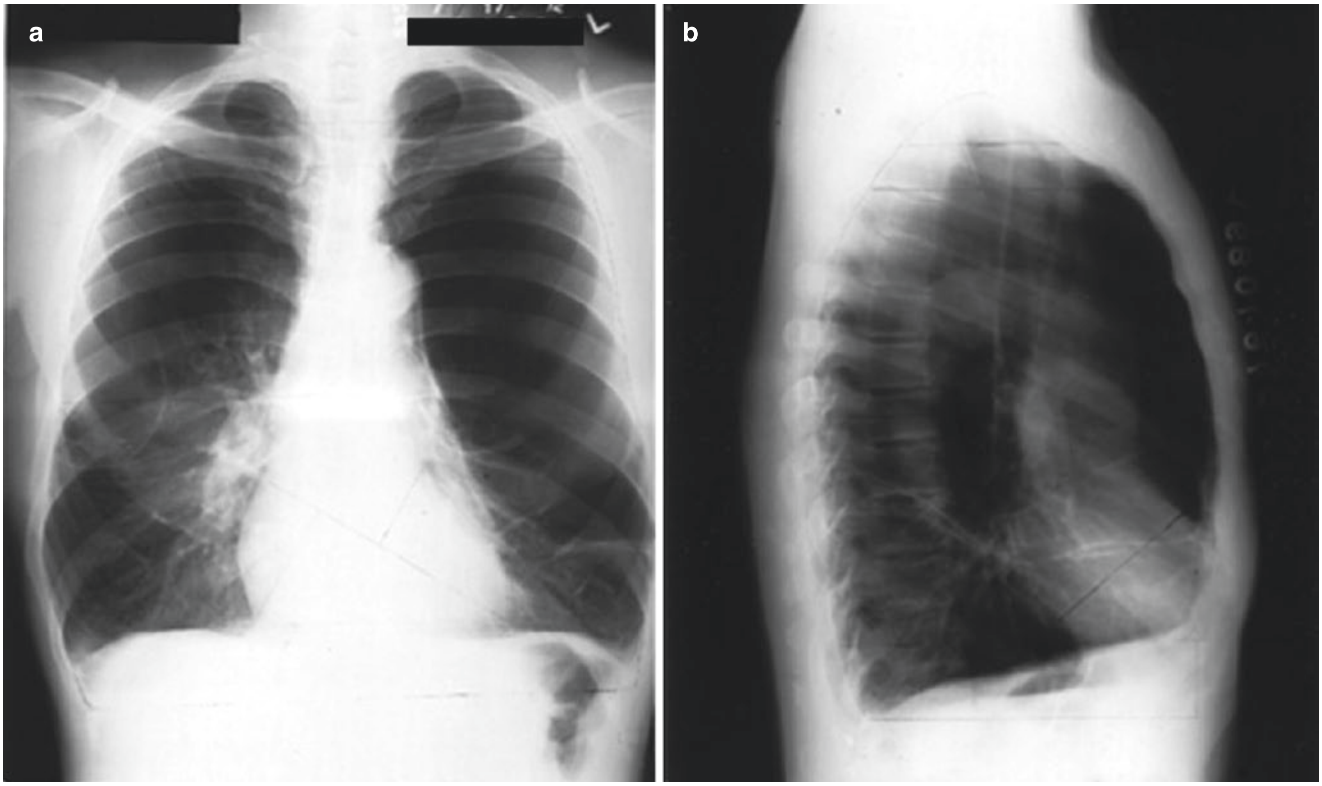

Fig. 3.5 (**a**) Shows a patient with emphysema. There is a marked hyperinflation with an increase in the anterior–posterior diameter of the chest. Also, there are flattening of the diaphragm bilaterally and generalized increase in the blackness of the film. (**b**) Shows the same patient a lateral chest X-ray

Many of the cases of emphysema seen in adult patients are strongly associated with cigarette smoking. The most striking image in a patient with advanced emphysema is a marked hyperinflation with an increase in the anteroposterior diameter of the chest, flattening of the diaphragmatic surfaces, and a generalized increase in the blackness of the film. Also there is a change in the vascular pattern, with attenuated vessels thinned and spread apart.

Often bullous areas are noted as large thin-walled air cysts, especially the apices. A bulla is defined as an air-filled space 1 cm or greater in diameter within the lung parenchyma that forms as a result of this destructive process. Rarely, one or more bullae enlarge to such a degree that they occupy more than one-third of the hemithorax. The term giant bullae is then applied. These easily distensible reservoirs are preferentially filled during inspiration, causing the collapse of adjacent, more normal lung parenchyma [12, 13]. Figure 3.5a shows a patient with emphysema, and Fig. 3.5b shows a lateral chest radiograph of the same patient. Figure 3.6 shows a PA chest X-ray and lateral radiograph of a patient with bullae. Figure 3.7 displays the chest X-ray showing a giant bulla occupying more than two-thirds of the right hemithorax and compressing the underlying lung.

Pneumothorax

Pneumothorax is the presence of air in the pleural space that is between the lung and the chest wall. Primary pneumothoraces arise in otherwise healthy people without any lung disease. Secondary pneumothoraces arise in subjects with underlying lung disease. Despite the absence of underlying pulmonary disease in patients with primary pneumothorax, subpleural blebs and bullae are likely to play a role in the pathogenesis. It is frequently the result of trauma, although sometimes the source of air leak cannot be readily detected.

The radiographic diagnosis of pneumothorax is usually straightforward. A visceral pleural line is seen without distal lung markings. On standard lateral views, a visceral pleural line may be seen in the retrosternal position or overlying the vertebrae, parallel to the chest wall [14, 15].

Pneumothoraces present as appearances on lateral chest radiographs; although the value of expiratory views is controversial, many clinicians still find them useful in the detection of small pneumothoraces when clinical suspicion is high and an inspiratory radiograph appears normal. The British Thoracic Society guidelines divide pneumothoraces into small and large based on the distance from visceral

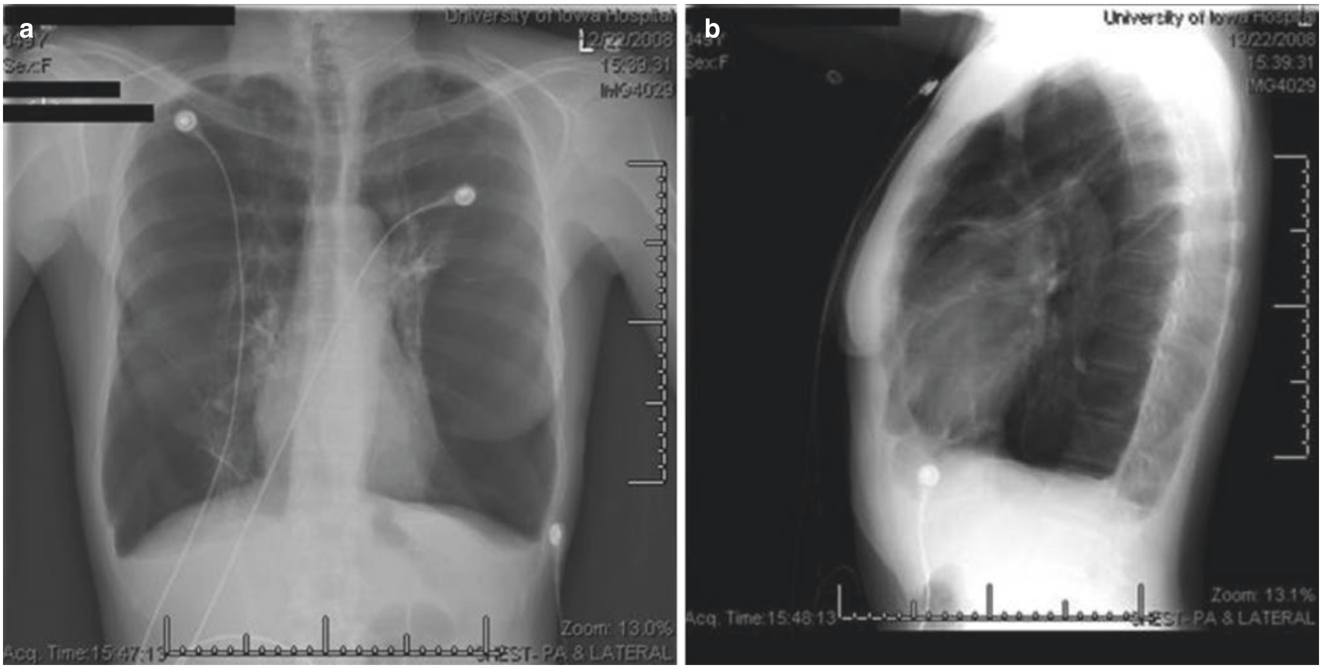

Fig. 3.6 (**a**) Shows a posterior–anterior chest X-radiograph of a patient with a bullae on the left hemithorax. (**b**) Shows the same patient on the lateral radiograph

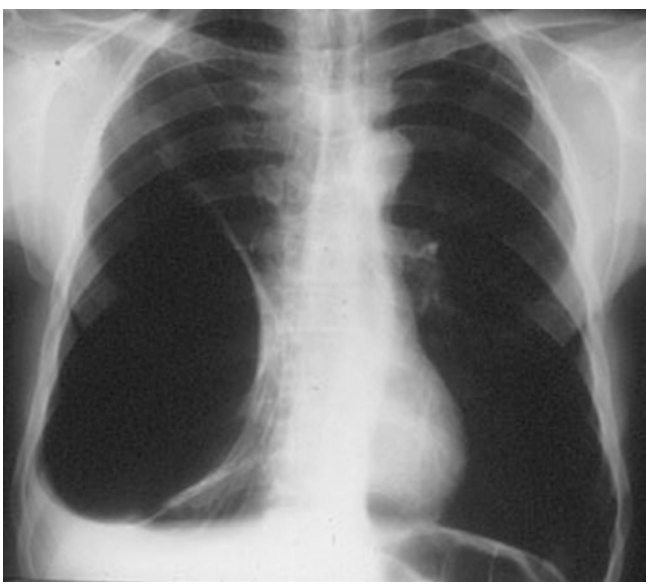

Fig. 3.7 Displays the chest X-ray showing a giant bullae occupying more than two-thirds of the right hemithorax and compressing the underlying lung

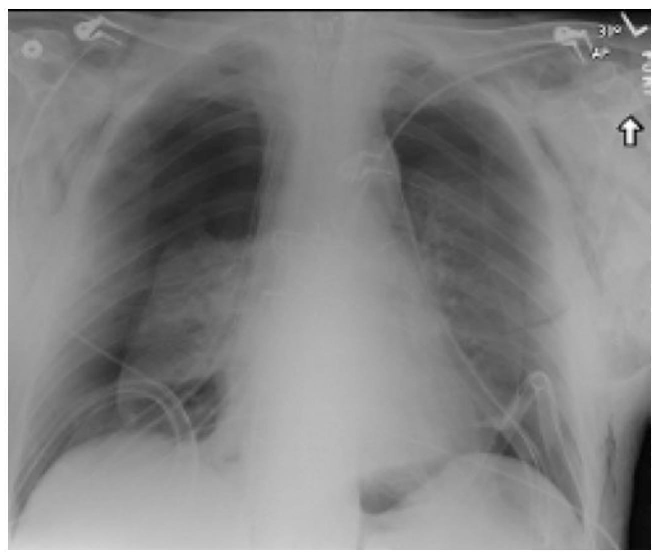

Fig. 3.8 Shows the chest radiograph of a patient with right-sided pneumothorax and bilateral chest tubes

pleural surface (lung edge) to chest wall, with less than 2 cm being small and more than 2 cm large [16]. A small rim of air around the lung actually translates into a relatively large loss of lung volume, with a 2-cm-deep pneumothorax occupying about 50% of the hemithorax.

In the supine position, air in the pleural space will usually be most readily visible at the lung bases in the cardiophrenic recess and may enlarge the costophrenic angle. Figure 3.8 shows the chest radiograph of a patient with right-sided pneumothorax.

Several well-known artifactual appearances can mimic the presence of a pneumothorax and should always be remembered during evaluation of chest radiography. The medial border of the scapula can imitate a lung edge but once considered can be traced in continuity with the rest of the bone, revealing its true nature. Skinfolds overlying the chest wall can simulate a visceral pleural line and, with the relative lack of lung markings in the upper zones, can lead to erroneous diagnosis. Once considered, however, the true nature of the image is readily apparent. Skinfolds are usually seen to pass outside the chest cavity, are straight or only minimally curved, and do not run parallel to the chest wall as with a true visceral pleural line. Skinfolds also form a dense line that is sharp on one side and blurred on the other in contrast to the less dense visceral pleural line. Also, radiopaque lines are often seen accompanying the inferior margins of ribs, which may simulate a visceral pleural line. These are often called companion shadows although some restrict this term to densities accompanying the first and second ribs. They are caused by protruding extrapleural fat or the subcostal grove.

Tension pneumothorax occurs when the intrapleural pressure exceeds the atmospheric pressure throughout inspiration as well as expiration. It is thought to result from the operation of a one-way valve system, drawing air into the pleural space during inspiration and not allowing it out during expiration. The development of tension pneumothorax is often, but not always, heralded by a sudden deterioration in the cardiopulmonary status of the patient related to impaired venous return, reduced cardiac output, and hypoxemia. The development of tension in a pneumothorax is not dependent on the size of the pneumothorax, and the clinical scenario of tension pneumothorax may correlate poorly with chest radiographic findings [17, 18]. In extreme cases of tension pneumothorax, the air leak brings about significant displacement of the mediastinum and contralateral lung into the opposite hemithorax causing significant hemodynamic instability.

Pleural Effusion

Pleural effusion does not involve the lung parenchyma; it can be the source of a significant amount of absorbing material in the path of the X-ray beam, causing opacity on the films. Large pleural effusions are easy to spot on a chest radiograph, but small pleural effusions can be overlooked easily, especially on portable films because the patients are almost always supine or semierect, and the fluid can collect either in a subpulmonic location or deep in the posterior costophrenic sulcus where it is hidden from view. Most often smaller effusions are seen as a veil-like opacity that is most pronounced at the base and tapers toward the lung apex. Figure 3.9 shows a male patient with a large pleural effusion of the left hemithorax occupying two-thirds of the chest cavity on the left side.

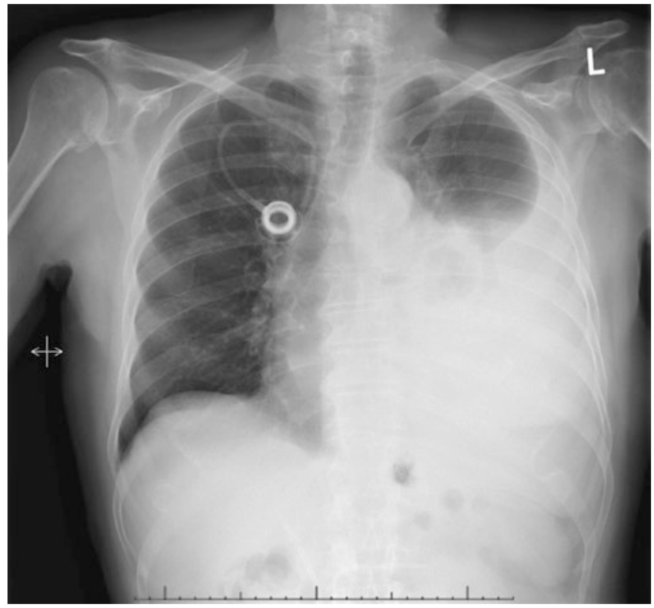

Fig. 3.9 Shows a male patient with a large pleural effusion on the left hemithorax occupying two-thirds of the chest cavity on the left side. Also there is the presence of an infusion port device on the right hemithorax

Chest Tube Placement

In general, appropriate use of chest tubes results in complete drainage of the collected air and fluid in the pleural space and allows full expansion and occupation of the entire pleural space by the lung, thus protecting the lung and pleural space from subsequent complications. Chest tubes are used routinely in the thoracic surgical patient. In practice, there are three main types that are used: (a) the large-caliber chest tube that involves the use of a 20–30 F size, (b) the small-caliber tube, and (c) the pigtail catheters. The typical and most common tubes have a side hole and end hole, and, in addition, they have an opaque marker that can be clearly seen in the chest X-radiograph. Many of those chest tubes can be inadvertently placed either in the major fissure, in lung parenchyma, or too high in the apex, and this can cause severe pain or damage to the lung.

In order to evaluate the position of a chest tube, an anterior–posterior chest radiograph or lateral films are useful [19]. In some circumstances, computed tomography (CT) scans of the chest are valuable for assessing chest tube position, for example, when misplacement is suspected but not confirmed on a plain radiograph [20]. Figure 3.10 shows a chest tube in a female patient placed in the right hemithorax.

Surgical emphysema is a well-known complication of intercostal tube drainage [21]. The development of surgical

Fig. 3.10 Shows a chest tube on the right hemithorax. The tip of the tube can be clearly seen at the level of the 6th intercostal space. Also, there is a PIC line going from a vein in the right arm to the entrance of superior vena cava

emphysema associated with pneumothorax involves an air-filled space, not formerly in communication with the subcutaneous tissue, being brought into communication with subcutaneous tissue. This may occur in the presence of a malpositioned, kinked, blocked, or clamped tube. Likewise, a small tube in the presence of a very large leak may potentially cause surgical emphysema. Any malpositioned chest tube should be visible with the chest radiograph. If the emphysema results in airway obstruction or thoracic compression, it may lead to severe respiratory insufficiency. The treatment is usually conservative, but in life-threatening situations, skin incision decompression and insertions of large-bore modified subcutaneous chest drains have all been used successfully.

Previous Lobectomy

Resection of a segment of the lung will produce changes somewhat similar to segmental atelectasis in that a portion of the lung is no longer present, and the remaining segments of the lobe, and other lobes on that side, will expand to fill the space. The chest radiograph will show a displacement of the interlobar fissure and elevation of the diaphragm. There might be a displacement of the hilum. Often the most common sign of the surgery in the chest is the presence of fine metallic sutures on the pleural surface at the site of the resection and, if it is an acute resection (after surgery), the presence of a chest tube. Also, an osteotomy of a rib can be seen in the chest radiograph.

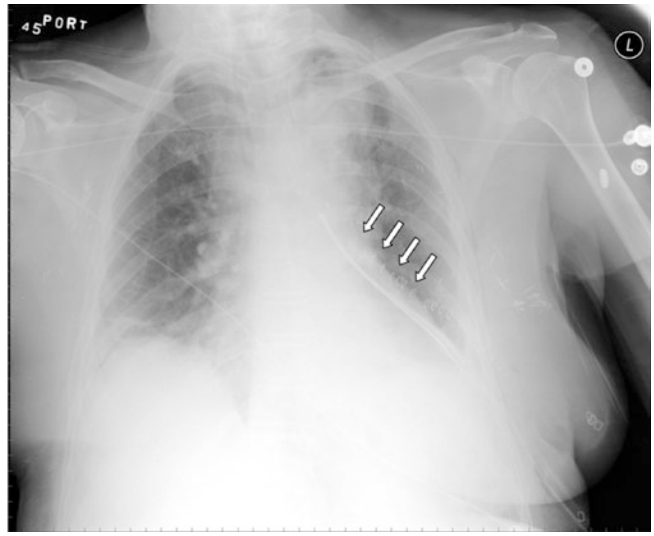

Fig. 3.11 Shows a chest X-ray of a female patient who had a left lower lobe lobectomy. The arrows are pointed to where the stapling line is. Also, there is a bilateral infiltrates postlobectomy

The lobectomy patient will often lead to a greater initial deformity of the involved hemithorax and some shift of the midline structures. As in cases of atelectasis, there should be compensatory overinflation of the noninvolved lobes. Figure 3.11 shows a chest X-ray of a female patient who had a left lower lobe lobectomy.

An important piece of information after lobectomy is the juxtaphrenic peak sign indicating upper lobe collapse. This is a common finding on chest radiographs of patients after upper lobectomy. It is more frequently seen after right upper lobectomy than after left upper lobectomy, and it is more often seen on erect than on supine radiographs. A study has shown that a juxtaphrenic peak can be expected to appear on chest radiographs in about 70% of patients 1 month or more after right upper lobectomy and in 50% after left upper lobectomy [22]. Figure 3.12 shows a patient who had a right upper lobectomy showing a thin juxtaphrenic peak.

Pneumonectomy

Removal of an entire lung leads to more drastic radiographic changes that evolve with the passage of time. Initially the affected side shows expected postoperative changes at the hilum and chest wall with a complete absence of lung tissue, leaving a very stark, air-filled cavity with extremely sharp

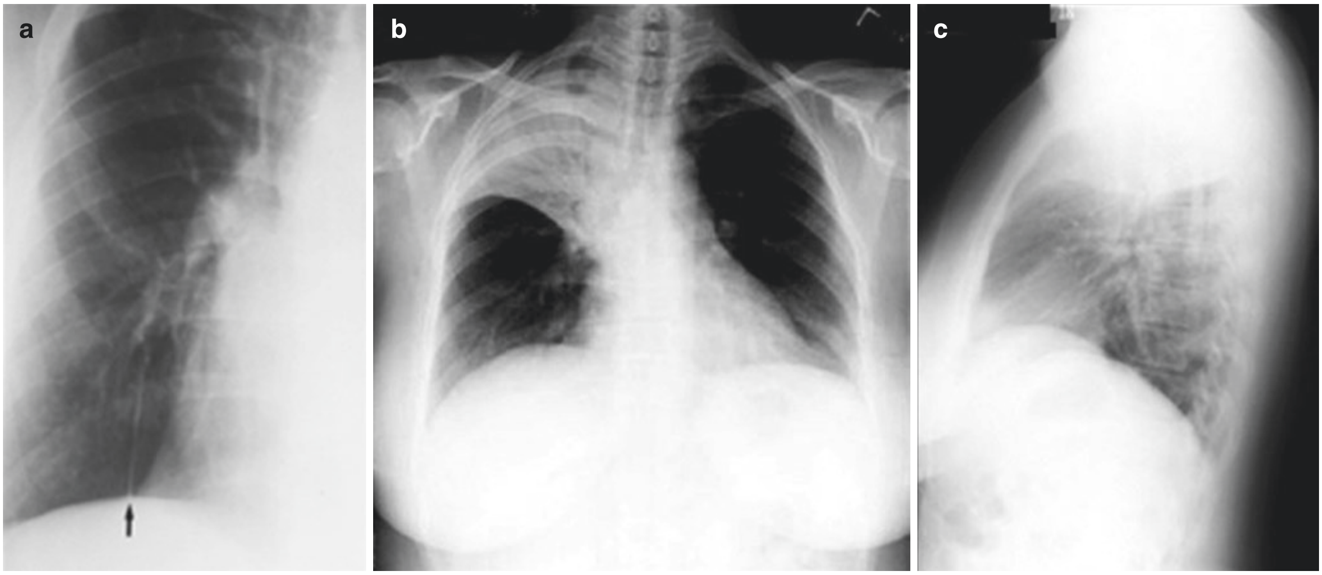

Fig. 3.12 (**a**) Shows a patient who had a right upper lobectomy showing a thin juxtaphrenic peak pointed with an arrow. (**b**) Shows a right upper lobectomy without the juxtaphrenic line. (**c**) Shows the same patient with the lateral chest radiograph

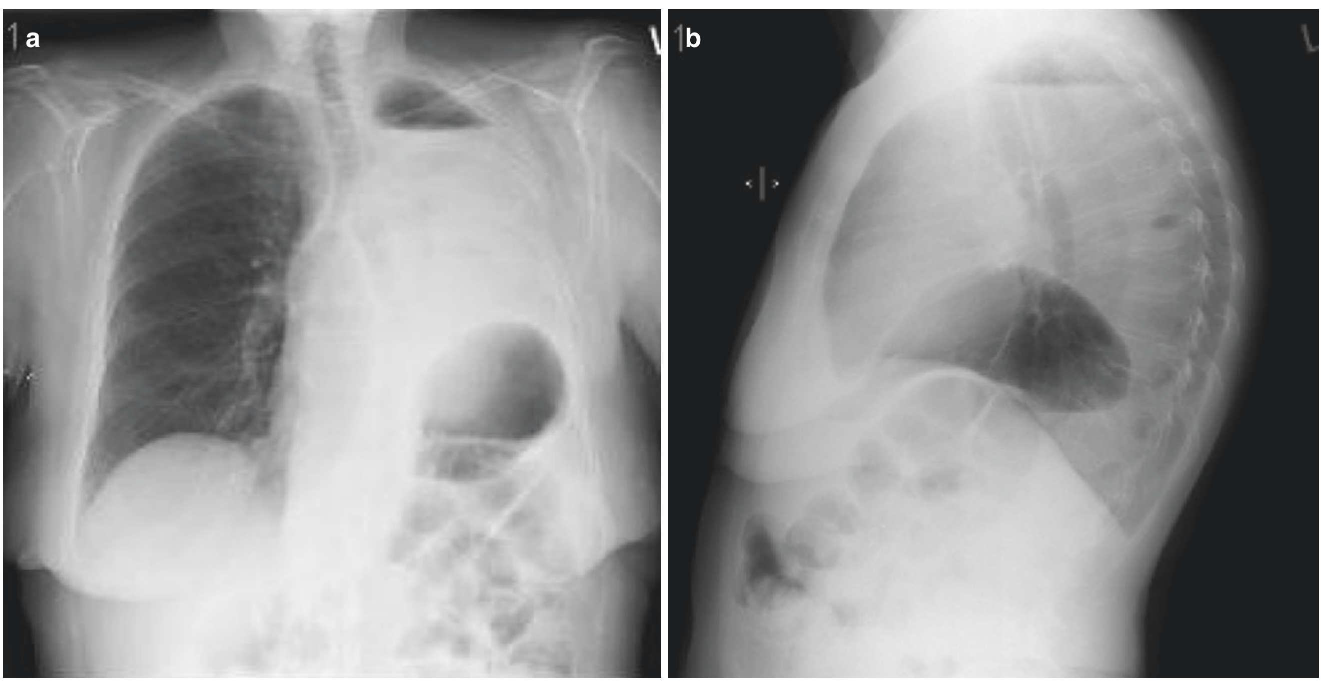

Fig. 3.13 (**a**, **b**) Shows a chest radiograph in anterior–posterior and lateral position in a patient with a left-sided pneumonectomy. On the left hemithorax, the white image corresponds to fluid in the hemithorax

margins of the heart and diaphragm. After pneumonectomy, air in the operated hemithorax is gradually reabsorbed and replaced by fluid with a net volume loss. As a result, the trachea and mediastinum gradually shift toward the surgical side. In the immediate postoperative period, a mediastinal shift away from the surgical side indicates atelectasis of the contralateral lung or an abnormal accumulation of air or fluid on the surgical side [23]. A rapid mediastinal shift can signify the presence of an air leak with a "ball valve" effect leading to a tension pneumothorax. There are usually some elevation of the hemidiaphragm and a shift of the heart and other midline structures toward the operated side as the remaining lung expands to take some of the space. Gradually the hemithorax fills with fluid, showing a distinct air fluid level if the patient is upright, or a more subtle increase in opacity if the patient is in the supine position. Figure 3.13

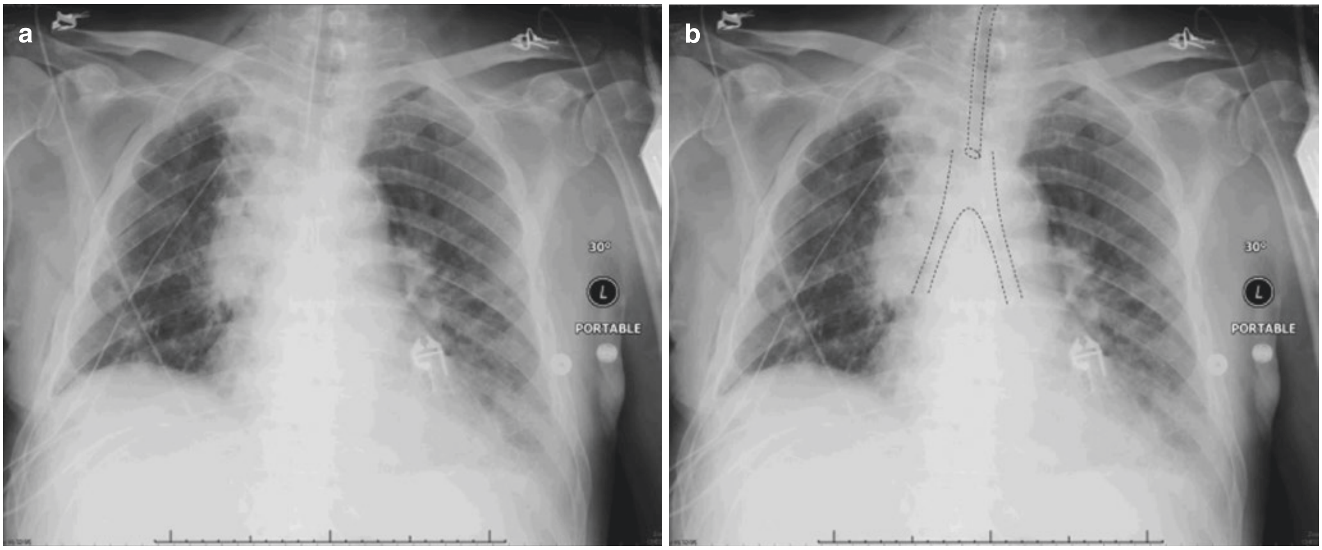

Fig. 3.14 (**a**) Shows a male patient who underwent a right upper lobectomy and remained intubated in the postoperative period with a single-lumen endotracheal tube. (**b**) Shows the same patient with a reconstruction of the single-lumen endotracheal tube. Notice that the tip of the single-lumen endotracheal tube should be placed 3 cm above the tracheal carina

shows a chest radiograph in anterior, posterior, and lateral position in a patient with a left-sided pneumonectomy.

After a thoracic surgical procedure, a chest radiograph film is required in order to assess lung expansion and chest tube placement, and if the patient remains intubated, the proper placement of the endotracheal tube must be assessed. The proper position of a single-lumen endotracheal tube as seen in the chest radiograph is that the distal tip of the tube is located approximately 3 cm above the tracheal carina. All endotracheal tubes have opaque markers that can be clearly identified in the radiographs. Figure 3.14a shows a male patient that underwent a right upper lobectomy and remained intubated in the postoperative period with a single-lumen endotracheal tube. Figure 3.14b shows the same patient with a reconstruction of the single-lumen endotracheal tube.

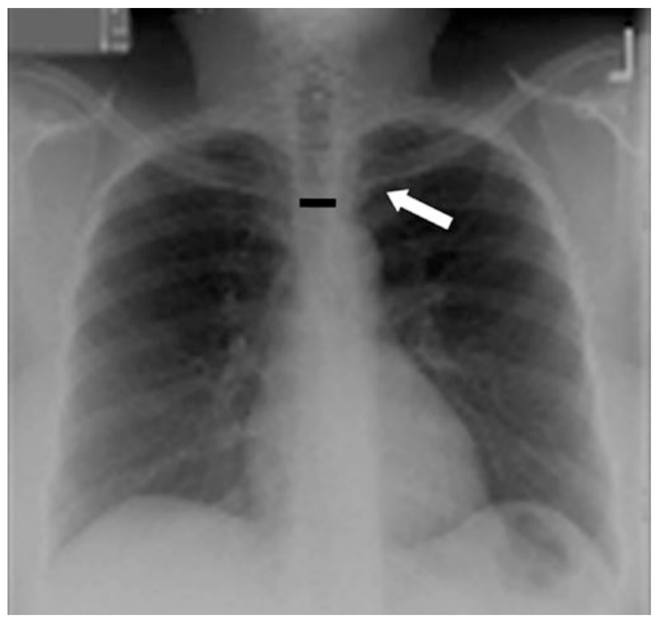

Fig. 3.15 Shows the measurement of the tracheal width at the level of the clavicles to estimate the proper size of the left-sided DLT from a chest radiograph

Double-Lumen Endotracheal Tubes

With any thoracic surgical procedure involving lung isolation devices, the anesthesiologist must review the tracheobronchial anatomy in the preoperative visit to determine whether or not abnormal anatomy exists. A view of the posteroanterior chest radiograph will allow assessment of the shadow of the tracheobronchial anatomy along with the bronchial bifurcation. It is estimated that in 75% of the films, the left mainstem bronchus shadow is seen. In addition, the chest radiograph can be useful to determine the proper size of a left-sided DLT. Brodsky et al. [24] reported that measurement of the tracheal diameter at the level of the clavicle on the preoperative posteroanterior chest radiograph can be used to determine proper left-sided DLT size (refer to Chap. 16). Figure 3.15 shows the measurement of the tracheal width at the level of the clavicles to estimate the proper size of the left-sided DLT from a chest radiograph. In addition, the chest radiograph will allow the visualization of the already placed DLT. The tip of each lumen is identified with a radiopaque marker. Figure 3.16a shows the chest radiograph of a patient with a left-sided

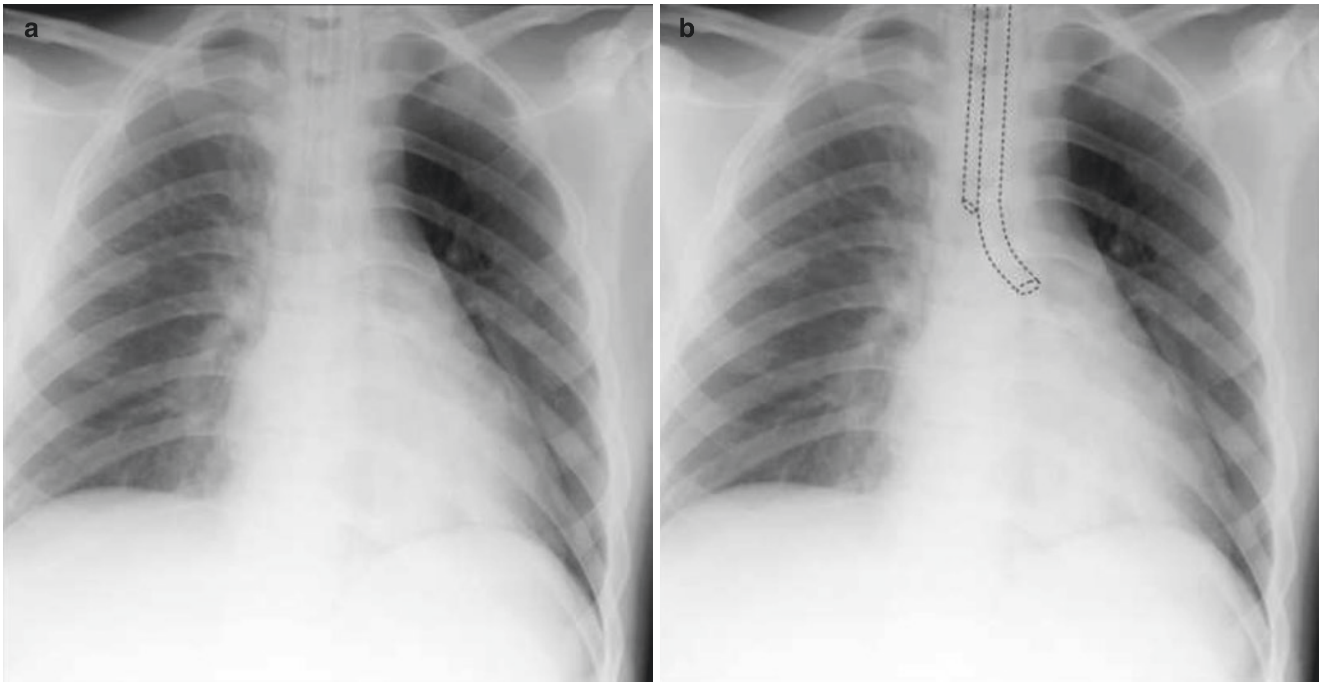

Fig. 3.16 (**a**) Shows the chest radiograph of a patient with a left-sided DLT in place. Notice the endobronchial lumen is approximately 2 cm below the tracheal carina into the left mainstem bronchus. (**b**) Shows a reconstruction of the DLT which is marked in the chest radiograph

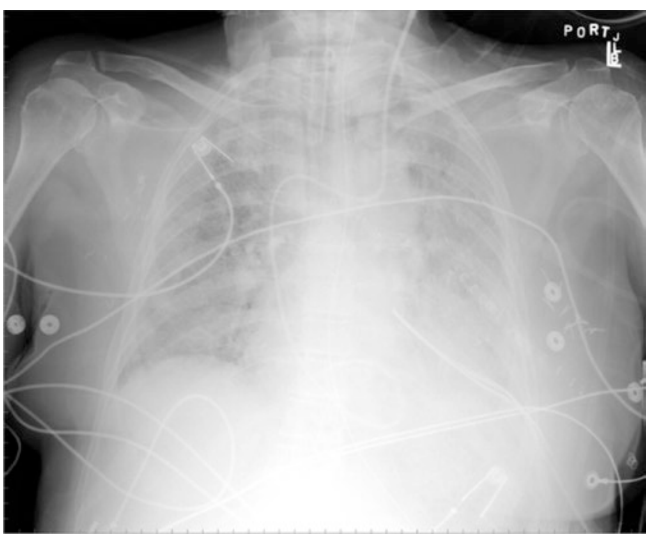

Fig. 3.17 Shows a patient with an acute lung injury (ALI) 72 h after the interstitial edema has progressed in the chest X-radiograph. There is a single-lumen endotracheal tube in place; also a pulmonary artery catheter introduced via the left internal jugular vein is seen. The chest radiograph also shows bilateral diffuse fluffy opacities typical of interstitial pulmonary edema postlobectomy

DLT in place. Notice the endobronchial lumen is approximately 2 cm below the tracheal carina into the left mainstem bronchus. Figure 3.16b shows a reconstruction of the DLT which is marked in the chest radiograph.

Postoperative Acute Lung Injury

Acute lung injury (ALI) may complicate thoracic surgery and is a major contributor to postoperative mortality. The incidence of ALI after thoracic surgery is estimated to be 4.2% [25, 26]. In a study by Licker et al. [25], they found a biphasic distribution pattern of ALI after lung resection. The primary form developed within the first 3 days after surgery and a secondary form triggered the onset of ALI after the third postoperative day.

The clinical presentation is a severe respiratory insufficiency with a progressive hypoxemia that does not respond to a conventional treatment including O_2 therapy. The chest radiograph of a patient with an ALI appears as patchy, unilateral or bilateral infiltrates, dependent pulmonary edema. In addition, atelectatic zones can be seen in the chest radiograph. Figure 3.17 shows a 60-year-old female following a left lower lobectomy who developed ALI in the immediate postoperative period; on the chest radiograph taken after 72 h, the interstitial edema has progressed. There is a single-lumen endotracheal tube in place; also a pulmonary artery catheter introduced via the left internal jugular vein can be seen. The chest radiograph also shows bilateral diffuse fluffy opacities typical of interstitial pulmonary edema postlobectomy after ALI.

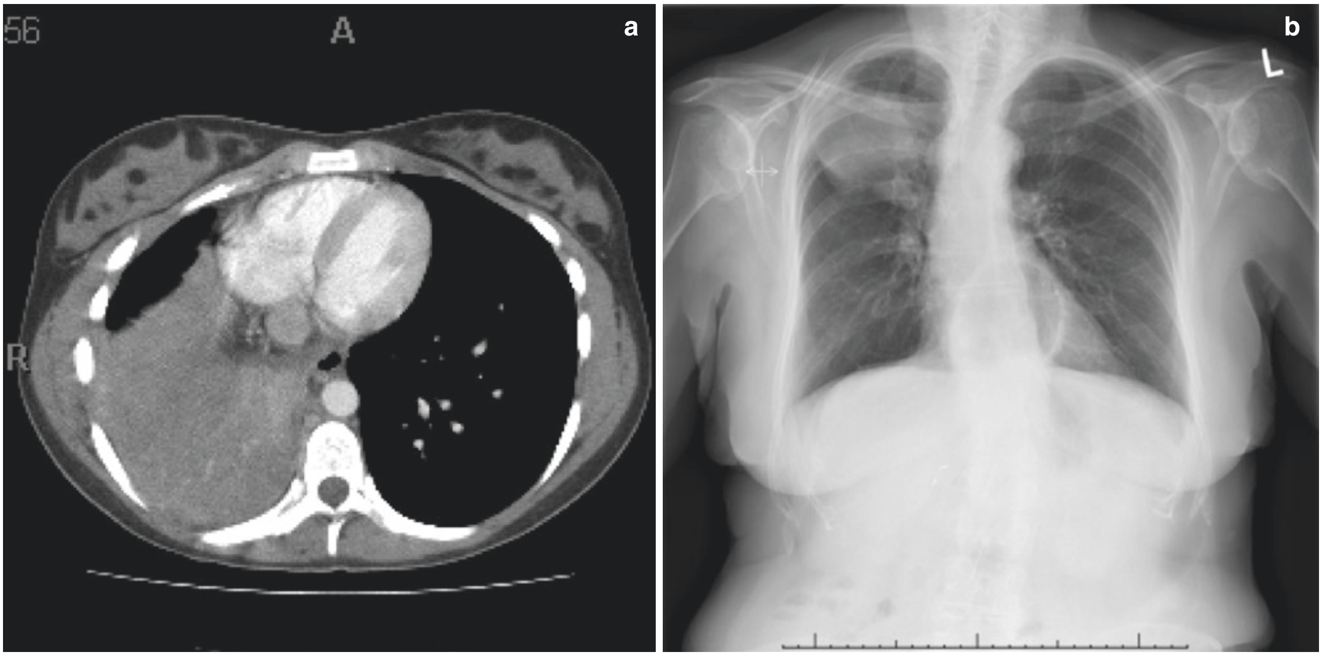

Fig. 3.18 (**a**) Shows a computed tomography (CT) scan of the chest. Diagnosis of pseudotumor of the lung. (**b**) Shows the chest radiograph showing the lung mass in the right upper lobe in the same patient. Diagnosis of right upper lobe adenocarcinoma

Computed Tomography Scan and Pulmonary Disease

CT scan of the chest is used as a diagnostic study; this is usually done after abnormal findings on a standard chest radiograph [27]. Common indications of CT include staging of lung cancer, solitary pulmonary nodule, mass or opacity, diffuse infiltrative lung disease, widened mediastinum, mediastinal mass, or other abnormalities of the mediastinum pleural abnormities, chest wall lesions, trauma, etc. Also, CT provides valuable information for the clinician with regard to the airway compression at any level of the tracheobronchial tree, as well as vascular compression diagnosis [28–31].

CT scans are performed in deep inspiration and at total lung capacity. For a routine helical CT of the chest, 2.5–5 mm sections are usually recommended. Thinner (1–2.5 mm) sections can be used to study fine details of the lung parenchyma. On routine studies, the field of view is adjusted to the size of the thorax, but small fields of view may be selected for smaller anatomic parts that require study. In addition, a contrast CT scan is useful in suspected vascular abnormalities such as pulmonary embolism. Recent improvements in scanner technology have led to the introduction of spiral or helical volumetric CT.

Computed Tomography Scan and Lung Mass, Mediastinal Mass, Pleural Effusion, and Pericardial Effusion

CT scan of the chest will confirm the presence of a mass in the chest and in many instances the specific location. Figure 3.18a shows a CT scan of the chest. There is the presence of a lung mass on the right lung. Figure 3.18b shows the chest radiograph showing the lung mass in the right upper lobe in a female patient. In addition, the CT scan of the chest will define the precise size and location of the mediastinal mass, any involvement with adjacent structures, as well as the degree of compression of the airway (trachea and/or bronchi). It is important during the assessment of the CT scan to identify the location of the mass, define its relationship to adjacent structures, assess the extent and degree of tracheal and/or vascular compression, and assess the patency of the airway at the tracheal and bronchial level. The CT scan also will permit accurate measurement of the airway diameter and will determine the precise level and extent of compression of the trachea. As mentioned previously, the average cross-sectional diameter of the trachea in a 70-kg, 170-cm tall person is approximately 18–23 mm. A tracheal diameter narrowing of 10 mm on CT corresponds to a 50% reduction in the tracheal cross-sectional area at that level. Figure 3.19 shows a CT scan of the chest with a large anterior mediastinal mass in the left hemithorax. Figure 3.20 shows a CT scan of the chest with a large anterior mediastinal mass on the left side causing compression to the entrance of the left mainstem bronchus.

A CT scan of the chest allows precise location of the extrapulmonary fluid whether in the peripheral pleural space or the interlobar fissure. Figure 3.21 shows a CT scan of the chest showing a large pleural effusion on the left hemithorax. Also, the CT scan is very useful for the diagnosis of pericardial effusions, because the precise location can be identified with this method. Figure 3.22 shows a pericardial effusion; notice the fluid in the pericardial sac.

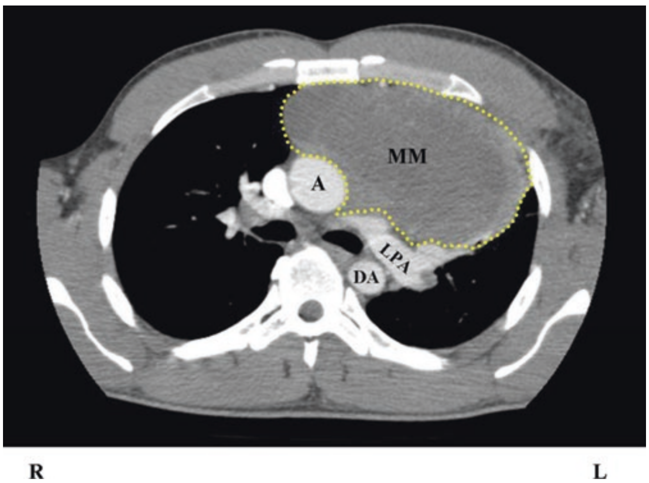

Fig. 3.19 Shows a computed tomography scan of the chest with a large anterior mediastinal mass on the left hemithorax (the dotted line is surrounding the mass). This patient has a diagnosis of mediastinal mass and diffuse B-cell lymphoma. MM mediastinal mass, LPA left pulmonary artery, A ascending aorta, DA descending aorta, R right, L left

In addition, a different alternative to assess the airways while using a CT scan is with the three-dimensional (3D) reconstruction of the airway using a workstation connected to a multidetector CT (MDCT) scanner. The MDCT provides high spatial resolution images of the whole lung without any anatomical gap. The technique consists of projecting the voxels with the lowest alteration value in every view through the volume explored, at various angles depending on the airway involved. If a tracheobronchial injury is suspected, 3D extraction of the airways may be useful by focusing the 3D volume-rendering technique to the tracheobronchial tree [32]. This technique is used for analyzing stenosis or distortion of the tracheobronchial tree but also may allow the diagnosis of tracheobronchial injury by demonstrating a wall defect and/or abnormal position of lobar and segmental bronchi [33, 34].

Also, a 3D scan of the chest is another modality to identify lymph nodes. The development of virtual bronchoscopy has led interest in introducing CT-based computer graphic techniques into the procedure of lung cancer staging. In virtual bronchoscopy, the 3D CT image serves as a high-resolution digital image replica of the chest [35]. Endoluminal renderings of the airways can be generated along paths following the airway central axes and lead to an off-line simulation of videobronchoscopy as virtual endoscopy; interior views are computer-generated from radiological images (see also Chap. 16, Fig. 16.14).

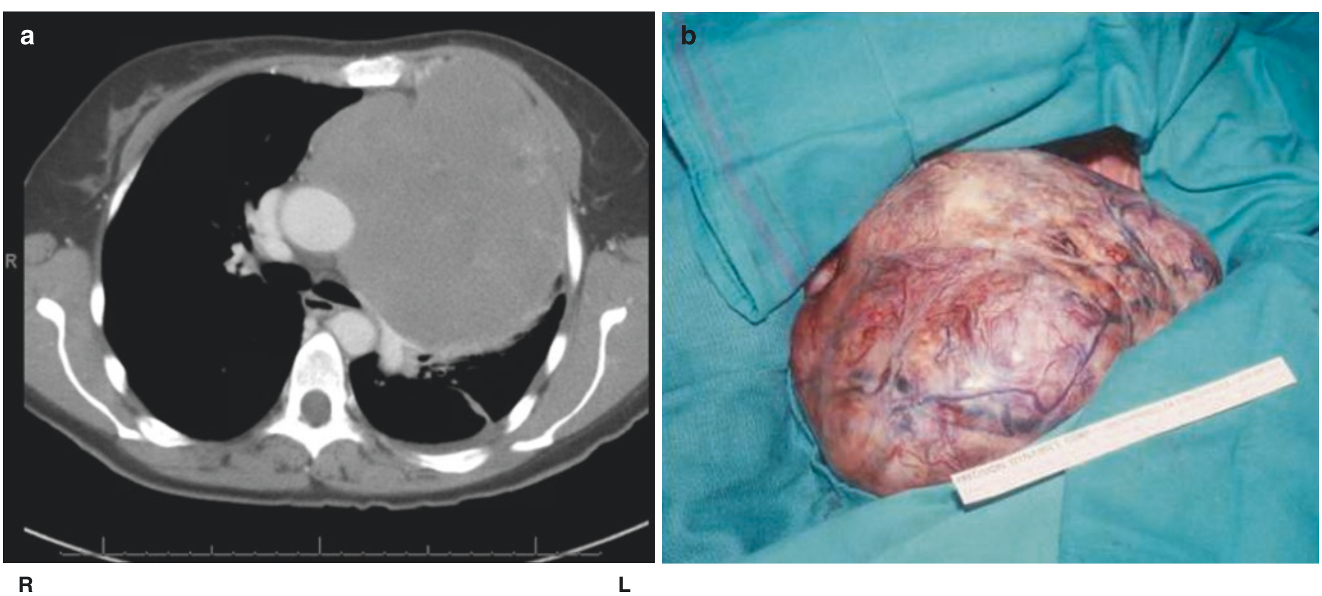

Fig. 3.20 (**a**) A computed tomography scan of the chest with a large anterior mediastinal mass on the left side causing compression to the entrance of the left mainstem bronchus. Diagnosis in this patient is germ cell tumor. (**b**) Showing a large mediastinal mass on left hemithorax

Fig. 3.21 Shows a CT scan of the chest showing a large pleural effusion on the left hemithorax. Also, the CT scan is very useful for the diagnosis of pericardial effusion, because of the precise location with this method

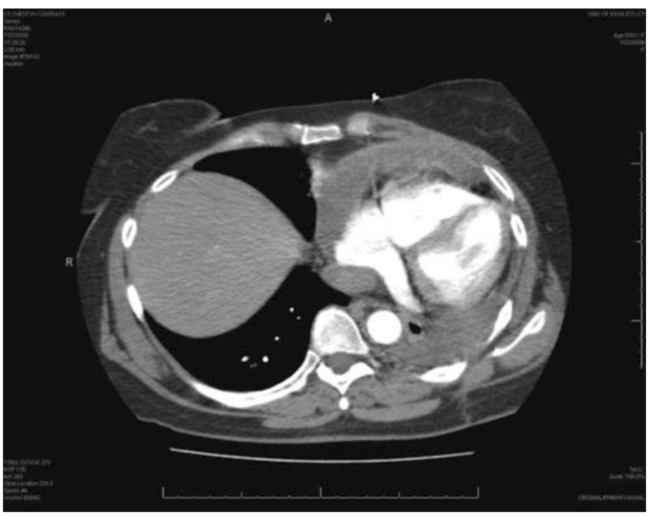

Fig. 3.22 Shows a pericardial effusion; notice the fluid in the pericardial sac

Imaging of the tracheobronchial tree has improved recently, in large part due to the advancement of CT, allowing for volumetric isotropic voxel imaging and its associated improvements in part processing software that allows for advanced three-dimensional (3D) visualization [36]. Thus airway imaging has become a tool that physicians can use to plan interventional procedures such as stent placement, surgery, and subsequent follow-up.

Patients undergoing thoracic surgical procedures who have large mediastinal mass with severe compromise of the airway require the placement of an airway stent; therefore, it is crucial to review CT scan in patients who have stent in place prior to surgery to assess the patency of the airway [37] (Fig. 3.23).

Multidetector Computer Tomography Scan of the Chest

Modern MDCT scanners readily provide very large high-resolution 3D volumetric images of the chest. Many 3D visualization techniques have been devised for more exhaustively viewing of the information contained in 3D MDCT chest images. The 3D MDCT image provides views of the segments of the airway tree, computes the central axes of the extracted airways, and also defines the endoluminal and exterior surfaces of the segmented airway tree and the exterior surfaces of the regions of interest for rendering [38].

One of the advantages of the MDCT and 3D reconstruction of the tracheobronchial tree is that it allows us to appreciate distorted tracheobronchial anatomy or changes in the airway with age. Figure 3.24 shows a MDCT scan of the chest on a male patient.

Magnetic Resonance Imaging and Pulmonary Disease

MRI produces images that superficially appear similar to CT scans. The MRI provides greater contrast resolution than CT scans and offers the potential for tissue characterization [39]. Also MRI of pulmonary parenchymal disease using a modified breath-hold 3D gradient echo technique allows imaging of a wide spectrum of solid and nonsolid pulmonary parenchymal diseases with reproducible high image quality, effective suppression of artifacts, and high resolution and visualization [40]. The 3D gradient echo technique allows better visualization of the peripheral and central parenchyma, pulmonary arteries, heart, and esophagus.

The MRI images are computer-generated images, usually in cross-sectional orientation but also with direct sagittal or coronal views, with tissues displayed in varying shades of black, white, and gray. MRI scans rely primarily on the evaluation of the amount of protons (water) in different tissues. This data information is acquired by placing the patient in a powerful magnetic field and interrogating the body with radio waves of a specific frequency and then listening for the response. By varying the frequency of the radio wave, the body can be imaged in multiple planes, not

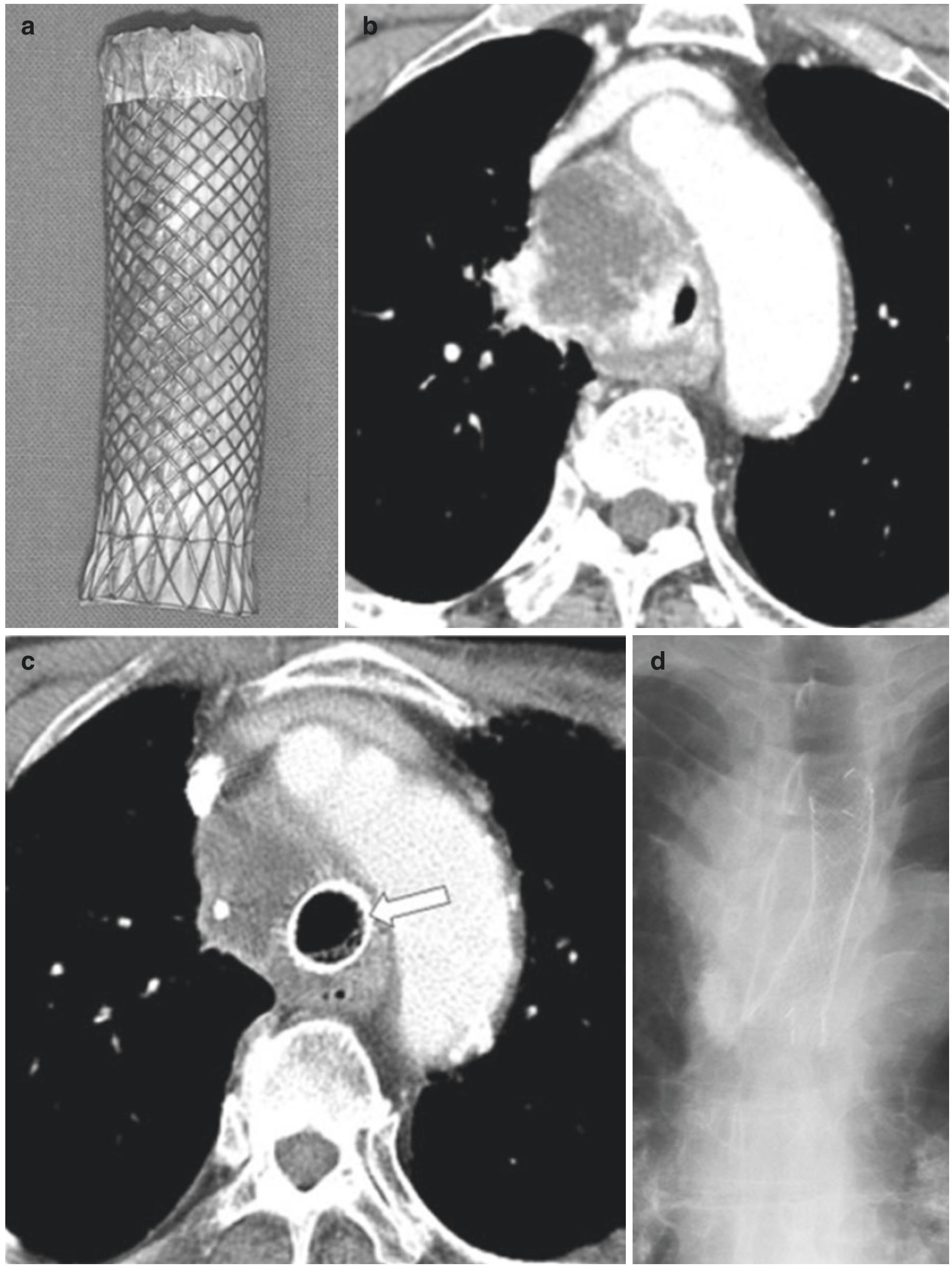

Fig. 3.23 Shows a tracheal stent in a patient with mediastinal mass. (**a**) Metallic expandable stent, (**b**) CT scan showing a mediastinal mass compressing the trachea, (**c**) airway stent in place seen by CT scan, (**d**) a chest X-ray showing the stent in place. (With permission Ref. [37])

just in axial sections. Direct sagittal and coronal images enable the radiologist to evaluate involvement of lung parenchyma [41], mediastinal structure, and the chest wall with greater clarity than with a CT scan. In addition, MRI is an adjunct to CT scan evaluation reserved for patients in whom CT scans did not resolve the anatomic issues or for whom additional information about the mediastinal and its relationship to other vital organs are required including invasion to heart or great vessels [30, 42, 43]. Figure 3.25 shows MRI of the chest in a patient with a mediastinal mass.

Fig. 3.24 Shows a multidetector computed tomography scan of the chest on a male patient

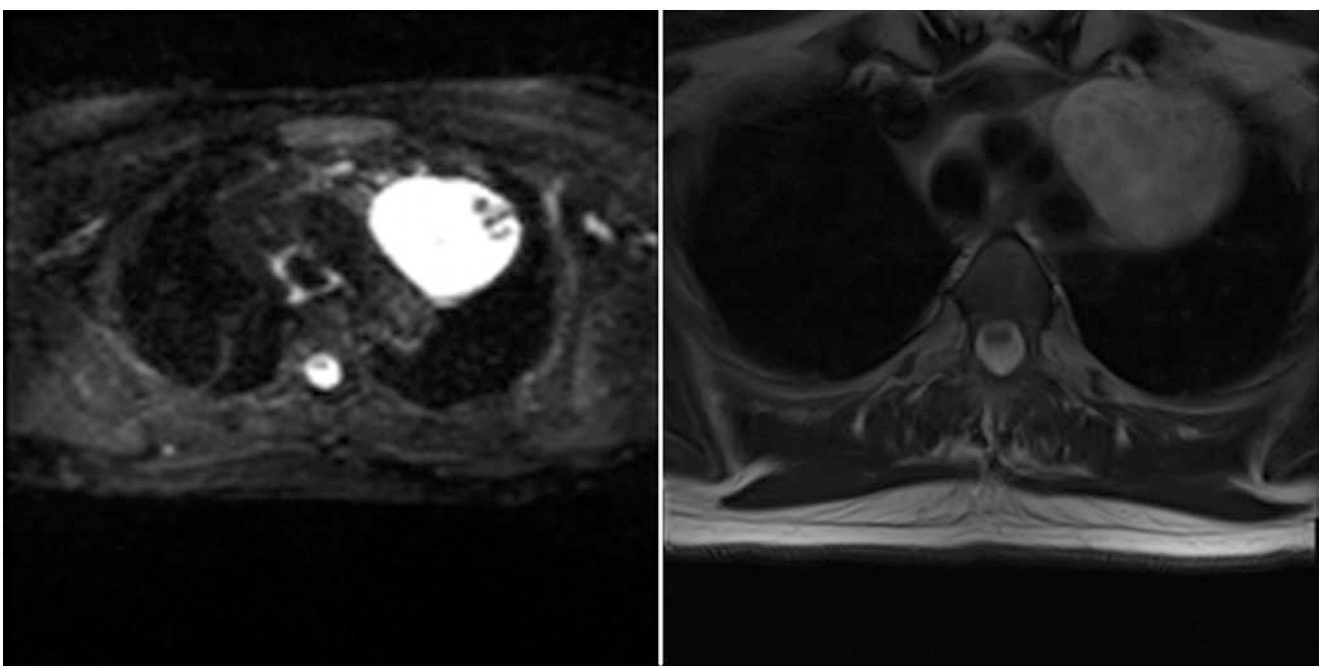

Fig. 3.25 Shows a magnetic resonance imaging of the chest in a patient with a mediastinal mass. This patient has a diagnosis of schwannoma

Summary

Radiological studies play an important role in the diagnosis and treatment of the thoracic surgical patient in the preoperative, intraoperative, and postoperative period. Chest radiographs allow us to identify distorted tracheobronchial anatomy, presence of lung masses, lung collapse, chest tube placement, endotracheal tube placement, and lung expansion or shifting of mediastinum in cases of tension pneumothorax. CT scans of the chest permit an identification and precise location of lung masses and mediastinal masses or the presence of fluid and compromise to adjacent structures; in addition it allows to identify the precise location of airway stents [44].

Multidetector computed tomography scan and 3D reconstruction allow identification of tracheobronchial anatomy in a more precise form. All radiological studies must be reviewed in the preoperative evaluation of thoracic surgical patients. In cases where the diagnosis or anatomy is unclear, these studies must be reviewed in conjunction with a thoracic surgeon or a radiologist.

References

1. Boiselle PM. Imaging of the large airways. Clin Chest Med. 2008;29:181–93.
2. Seymour AH. The relationship between the diameters of the adult cricoid ring and main tracheobronchial tree: a cadaver study to investigate the basis for double-lumen tube selection. J Cardiothorac Vasc Anesth. 2003;17:299–301.
3. Minnich DJ, Mathisen DJ. Anatomy of the trachea, carina and bronchi. Thorac Surg Clin. 2007;17:571–85.
4. Stene R, Rose M, Weigner MB, et al. Bronchial trifurcation at the carina complicating use of a double-lumen tracheal tube. Anesthesiology. 1994;80:162–1164.
5. Campos JH. Update on tracheobronchial anatomy and flexible fiberoptic bronchoscopy in thoracic anesthesia. Curr Opin Anaesthesiol. 2009;22:4–10.
6. Goldwin RL, Reed JC. Chapter 2: Radiology of the chest. In: Kaplan J, Slinger P, editors. Thoracic anesthesia. 3rd ed. New York: Churchill Livingstone; 2003. p. 24–56.
7. Fraser RS, Pare JA, Fraser RG, et al. Synopsis of diseases of the chest. 2nd ed. Philadelphia: WB Saunders; 1994.
8. Datt V, Tempe DK. Airway management in patients with mediastinal masses. Indian J Anaesth. 2005;49:344–52.
9. Ahmed-Nusrath A, Swanevelder J. Anesthesia for mediastinoscopy. Contin Educ Anaesth Crit Care Pain. 2007;7:6–9.
10. Campos JH. Chapter 11: Managing the patient with an anterior mediastinal mass In: Cohen NH, editor. Medically challenging patients undergoing cardiothoracic surgery, Society of Cardiovascular Anesthesiologists Monograph. Baltimore: Lippincott Williams & Wilkins; 2009. p. 285–302.
11. Harris GJ, Harman PK, Trinkle JK, et al. Standard biplane roentgenography is highly sensitive in documenting mediastinal masses. Ann Thorac Surg. 1987;44:238–41.
12. Morgan MDL, Edward CW, Morris J, et al. Origin and behavior of emphysematous bullae. Thorax. 1989;44:533–8.
13. Schipper PH, Meyers BF, Battafarano RJ, et al. Outcomes after resection of giant emphysematous bullae. Ann Thorac Surg. 2004;78:976–82.
14. O'Connor AR, Morgan WE. Radiological review of pneumothorax. BMJ. 2005;330:1493–7.
15. Glazer H, Anderson DJ, Wilson BS, et al. Pneumothorax: appearances on lateral chest radiographs. Radiology. 1989;173:707–11.
16. Henry M, Arnold T, Harvey J. BTS guidelines for the management of spontaneous pneumothorax. Thorax. 2003;58(Suppl 2):ii39–52.
17. Light RW. Tension pneumothorax. Intensive Care Med. 1994;20:468–9.
18. Baumann MH, Sahn SA. Tension pneumothorax: diagnostic and therapeutic pitfalls. Crit Care Med. 1994;22:896.
19. Symbas PN. Chest drainage tubes. Surg Clin North Am. 1989;69:41–6.
20. Baldt MM, Bankier AA, Germann PS, et al. Complications after emergency tube thoracostomy: assessment with CT. Radiology. 1995;195:539–43.
21. Maunder RJ, Pierson DJ, Hudson LD. Subcutaneous and mediastinal emphysema. Pathophysiology, diagnosis, and management. Arch Intern Med. 1984;144:1447–53.
22. Konen E, Rozenman J, Simansky DA, et al. Prevalence of the juxtaphrenic peak after upper lobectomy. Am J Roentgenol. 2001;177:869–73.
23. Wechsler RJ, Goodman LR. Mediastinal position and air-fluid height after pneumonectomy: the effect of the respiratory cycle. Am J Roentgenol. 1985;145:1173–6.
24. Brodsky JB, Macario A, Mark JB. Tracheal diameter predicts double-lumen tube size: a method for selecting left double-lumen tubes. Anesth Analg. 1996;82:861–4.
25. Licker M, de Perrot M, Spiliopoulos A, et al. Risk factors for acute lung injury after thoracic surgery for lung cancer. Anesth Analg. 2003;97:1558–65.
26. Hayes JP, Williams EA, Goldstraw P, et al. Lung injury in patients following thoracotomy. Thorax. 1995;50:990–1.
27. McLoud T. Chapter 36: Imaging the lungs. In: Patterson C, Deslauriers L, Luketich R, editors. Pearson's thoracic surgery. 3rd ed. New York: Churchill Livingstone; 2008. p. 415–28.
28. Harte BH, Jaklitsch MT, McKenna SS, et al. Use of a modified single-lumen endobronchial tube in severe tracheobronchial compression. Anesthesiology. 2002;96:510–1.
29. Slinger P, Karsli C. Management of the patient with a large anterior mediastinal mass: recurring myths. Curr Opin Anaesthesiol. 2007;20:1–3.
30. Chiles C, Woodard PK, Gutierrez FR, et al. Metastatic involvement of the heart and pericardium: CT and MR imaging. Radiographics. 2001;21:439–49.
31. Shepard JA, Grillo HC, McLoud TC, et al. Right-pneumonectomy syndrome: radiologic findings and CT correlation. Radiology. 1986;161:661–4.
32. Le Guen M, Beigelman C, Bouhemad B, et al. Chest computed tomography with multiplanar reformatted images for diagnosing traumatic bronchial rupture: a case report. Crit Care. 2007;11:1–8.
33. Rubin GD, Beaulieu CF, Argiro V, et al. Perspective volume rendering of CT and MR images: applications for endoscopic imaging. Radiology. 1996;199:321–30.
34. Boiselle PM, Reynolds KF, Ernst A. Multiplanar and three-dimensional imaging of the central airways with multidetector CT. Am J Roentgenol. 2002;179:301–8.
35. Higgins WE, Ramaswamy K, Swift RD, et al. Virtual bronchoscopy for three-dimensional pulmonary image assessment: state of the art and future needs. Radiographics. 1998;18:761–78.
36. Laroia AT, Thompson BH, Laroia ST, et al. Modern imaging of the tracheo-bronchial tree. World J Radiol. 2010;2:237–48.

37. Shin JH, Song HY, Ko GY, et al. Treatment of tracheobronchial obstruction with a polytetrafluoroethylene-covered retrievable expandable nitinol stent. J Vasc Interv Radiol. 2006;17:657–63.
38. Higgins WE, Helferty JP, Lu K, et al. 3D CT-video fusion for image-guided bronchoscopy. Comput Med Imaging Graph. 2008;32:159–73.
39. Moore EH, Webb WR, Muller N, et al. MRI of pulmonary airspace disease: experimental model and preliminary clinical results. Am J Roentgenol. 1986;146:1123–8.
40. Bader TR, Semelka RC, Pedro MS, et al. Magnetic resonance imaging of pulmonary parenchymal disease using a modified breath-hold 3D gradient-echo technique: initial observations. J Magn Reson Imaging. 2002;15:31–8.
41. Bergin CJ, Glover GH, Pauly JM. Lung parenchyma: magnetic susceptibility in MR imaging. Radiology. 1991;180:845–8.
42. Bremerich J, Roberts TP, Wendland MF, et al. Three-dimensional MR imaging of pulmonary vessels and parenchyma with NC100150 injection (Clariscan). J Magn Reson Imaging. 2000;11:622–8.
43. Bittner RC, Felix R. Magnetic resonance (RM) imaging of the chest: state-of-the-art. Eur Respir J. 1998;11:1392–404.
44. Marchese R, Poidomani G, Paglino G, et al. Fully covered self-expandable metal stent in tracheobronchial disorders: clinical experience. Respiration. 2015;89:49–56.